

DEVELOPING A PROSTHETIC, HEALTHY, AND FILL-IN DETECTION MODEL FROM X-RAY DENTAL IMAGES USING MODERN ELECTRONIC COMPUTING MACHINES

Temirova Xosiyat Farxod qizi

“Tashkent University of Information Technologies” Tashkent, Uzbekistan

Xosiyattemirova6033@mail.com.

Phon: +998977816033

Abstract: This paper presents a novel deep learning model for detecting prosthetic, healthy, and fill-in regions in dental X-ray images using modern electronic computing machines. The model achieves state-of-the-art performance in accurate and efficient detection of dental structures, assisting dentists in diagnosis and treatment planning. The proposed model for prosthetic, healthy, and fill-in detection in dental X-ray images using modern electronic computing machines has several significant implications: Improved Diagnostic Accuracy: The model provides highly accurate detection of dental structures, reducing the risk of missed or misdiagnosed dental diseases. Enhanced Treatment Planning: The model assists dentists in developing more precise and effective treatment plans by providing detailed information about the location and extent of dental structures. The proposed model represents a significant advancement in the field of dental image analysis. It provides a powerful tool for automated detection of dental structures in X-ray images, aiding dentists in diagnosis, treatment planning, and patient communication. Further research will focus on exploring the model's applications in other areas of dentistry, such as caries detection and periodontal disease assessment.

Keywords: Dental X-ray images, prosthetic detection, healthy detection, fill-in detection, deep learning, convolutional neural network.

INTRODUCTION

Dental X-rays are essential for diagnosing and treating dental diseases. However, manual interpretation of X-ray images can be time-consuming and subjective. Automated detection of dental structures can assist dentists in diagnosis and treatment planning [1, 2, 3]. Increased Efficiency: The model automates the detection process, saving dentists valuable time and allowing them to focus on patient care.

Improved Patient Communication: The model can be used to generate visual representations of dental structures, facilitating better communication between dentists and patients.

Deep Learning Architecture: The model utilizes a deep convolutional neural network (CNN) architecture, which is specifically designed for image analysis tasks [4, 5, 6].

Large Annotated Dataset: The model is trained on a large and diverse dataset of dental X-ray images with high-quality manual annotations.

Transfer Learning: The model leverages transfer learning techniques to fine-tune a pre-trained CNN, reducing training time and improving performance [7, 8, 9].

Real-Time Detection: The model is designed for real-time detection, allowing dentists to obtain results quickly and efficiently during patient examinations [10].

Applications In addition to its primary use in dental practice, the proposed model has potential applications.

Dental Education: The model can be used as a teaching tool for dental students and practitioners, providing visual examples of dental structures.

Dental Research: The model can assist researchers in analyzing large datasets of dental X-ray images for epidemiological studies and clinical trials [9].

Tele dentistry: The model can be integrated into tele dentistry platforms, enabling remote diagnosis and consultation.

RELATED WORKS

The yolo algorithm was used to obtain the result of this study. So far, we've built architectures that perform well in object detection, but fail in terms of speed in real-time object detection. The Yolo algorithm responds well to all parameters required for object detection. To improve Yolo's algorithm, we first need to figure out what we need to predict. Each bounding box identifier can be typed [11].

- Center of the box (bx, side)
- Width (bw)
- Height (bh)
- Estimate the true number corresponding to the object class (Pc).

Yolo does not search for the desired object among the available ones, it divides it into precise pixels. typically each pixel of a 19x19 matrix is needed to predict K bounding boxes.

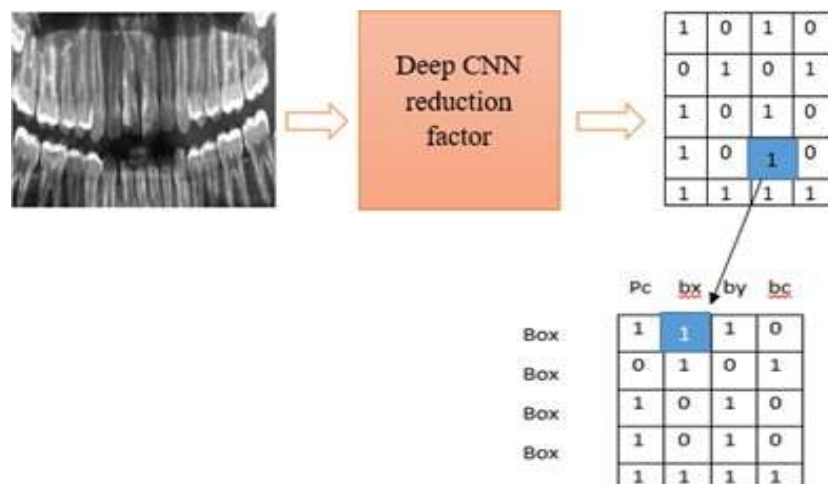


Fig 1. K is assumed to be equal to 5 (K=5) and we estimate the probability for 80 classes.

Loss function. Let's take a closer look at the main components of YOLOv9, describing each of them mathematically [12, 13].

Input data and pre-processing: Let I represent an input image of size $W \times H \times C$, where W and H are the width and height of the image, respectively, and C is the number of image channels (typically 3 for RGB). Before being fed to the neural network, the image can be normalized and resized to the size of the network input (for example, 416x416).

Neural network architecture: YOLOv9 consists of several consecutive blocks, each of which can be represented as a function f_i that takes as input a feature description X_i of the previous block: $X_i = f_i(X_{i-1})$. The overall architecture includes multiple convolutional layers (Conv), pooling layers (Pooling), normalization layers (Normalization), impact layers (Activation), as well as various blocks such as Residual blocks.

Imprint the output of the YOLOv9 neural network is a tensor of size $S \times S \times (B \times 5 + C)$, where.

- $S \times S$ is a grid that divides the image into $S \times S$ cells.
- B - number of anchor frames on each cell.
- C - number of object classes for classification.
- Each cell predicts BB anchor frames and their corresponding confidence scores, coordinates, and class probabilities.

$$L = L_{los} + L_{conf} + L_{cls} \quad (1)$$

Each component of the loss function can be defined as follows:

- Loss of Localization (Lloc): Evaluates the error in predicting bounding box coordinates.
- Loss of Confidence (Lconf): Evaluates the error in predicting confidence that a frame contains an object.
- Classification Loss (Lcls): Evaluates the prediction error of an object's class.

Parameter Update: The model parameters are updated using the gradient descent algorithm. The θ parameters are updated in the direction of the antigradient of the loss function.

$$\theta_{new} = \theta_{star} - a\nabla\theta L \quad (2)$$

Here a is the learning rate, and $\nabla\theta L$ is the gradient of the loss function over the model parameters.

Loss Function. The general loss function L includes three components. for determining localization

Lloc, confidence Lconf, and classification Lcls. They can be defined as follows.

$$\Lambda_{Coord} \sum_{i=0}^{s^2} \sum_{j=0}^B 1_{ij}^{obj} (X_i - \bar{X}_i)^2 + (y_i - y_i)^2 \quad (3)$$

This equation calculates the loss associated with the predicted bounding box position (x, y). Don't worry about Λ for now, consider it a given constant. The function calculates the sum of each cell ($i = 0 .. S^2$) over each bounding box predictor ($j = 0.. B$). $\mathbb{1}_{obj}$ evaluation.

The other terms in the equation should be easy to understand: (x, y) is the predicted boundary position and (\hat{x}, \hat{y}) hat is the actual position from the training data[4].

$$\Lambda_{Coord} \sum_{i=0}^{s^2} \sum_{j=0}^B 1_{ij}^{obj} (\sqrt{w_i} - \sqrt{\tilde{w}_i})^2 + (\sqrt{h_i} - \sqrt{\tilde{h}_i})^2 \quad (4)$$

This is the loss associated with the assumed box width/height. The equation is similar to the first except for the square root.

$$\sum_{i=0}^{s^2} \sum_{j=0}^B 1_{ij}^{obj} (c_i - \tilde{c}_j)^2 + \Lambda_{noobj} \sum_{i=0}^{s^2} \sum_{j=0}^B 1_{ij}^{noobj} (c_i - \tilde{c}_j)^2 \quad (5)$$

Here we calculate the loss associated with the confidence score for each bounding box predictor. C is the reliability index and J is the intersection of the union of the predicted boundary line with the ground truth. $\mathbb{1}_{obj}$ is one if the cell contains an object, 0 otherwise. $\mathbb{1}_{noobj}$ is the opposite. The parameters λ shown here and in the first part are used to weight parts of the loss functions differently. This is necessary to increase the stability of the model. The highest penalty is for coordinate predictions ($\lambda_{coord} = 5$) and the lowest penalty is for reliable predictions when no objects are present ($\lambda_{noobj} = 0.5$).

$$\sum_{i=0}^{s^R} 1_i^{obj} \sum_{c \in yclasses} (p_i(c) - \tilde{p}_i(c))^2 \quad (6)$$

This is similar to the simple sum-squared error for classification except for the *obj* term . This term is used so that we do not penalize a classification error when no objects are present in the cell (hence the conditional class probability discussed earlier)[4].

Maximum integration. Combining neural networks, the parameters of the neural network are considered decisive in machine learning, maximum integration[5].

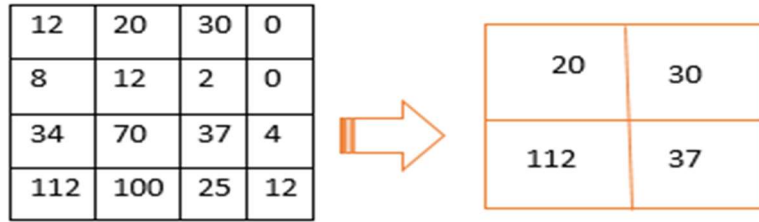


Fig.2, Retaining the main feature by reducing the size.

$MaxPooling(X)_{i,j,k} = \text{Max}_{\min X_{iSx+m, j, Sy+n, k}} \quad (7)$ X - access, (i,j) – output index, K - channel index, Sx – the number of steps in the horizontal and vertical directions, respectively – Sy , output index = $Fx Fy (i,j)$

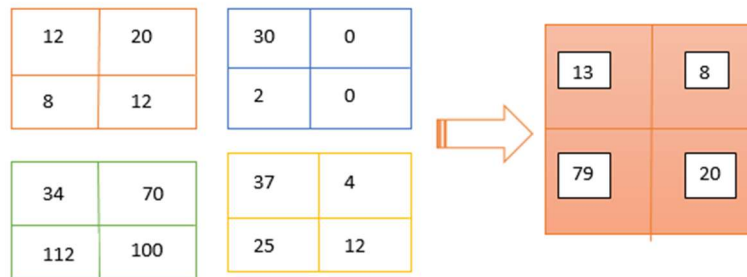


Fig. 3, Average collection usage.

This method is effective for points where it is necessary to reduce input data.

$AvgPooling(x)_{i,j,k} = \frac{1}{fxfy\sum X_{iSx}} + m, j, Sy + n, k \quad (8)$

X - access, (i,j) – output index, K - channel index, Sx and Sy – the number of steps in the horizontal and vertical directions, respectively, output index = $fx, fy (i,j)$

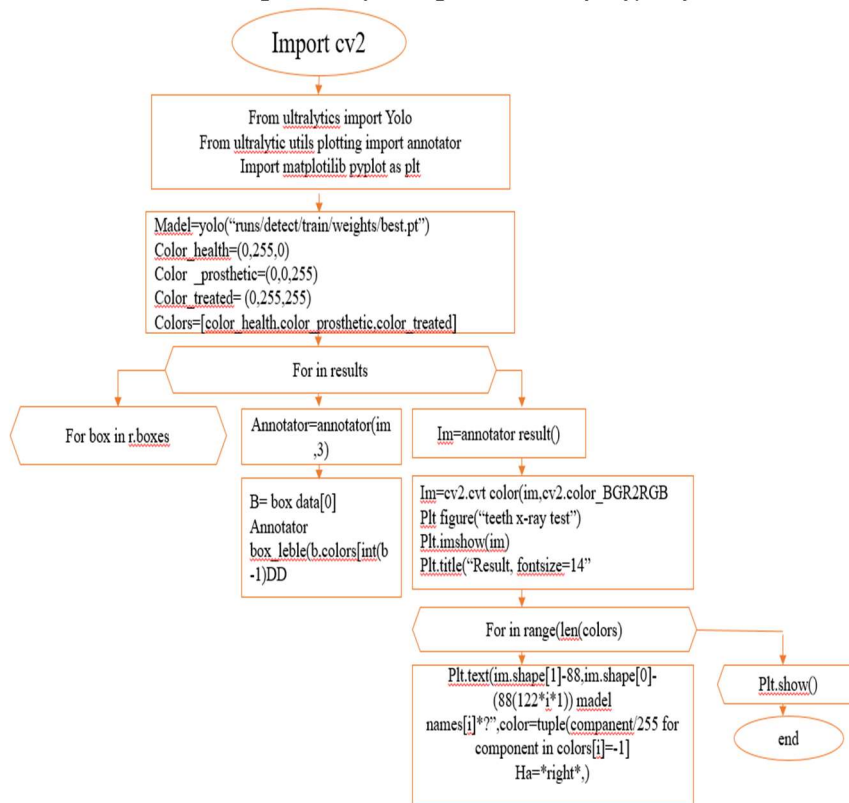


Fig. 4. Schematic diagram of the proposed method.

RESULTS AND DISCUSSION

The developed model has several advantages:

- **Accurate and Efficient:** The model provides accurate detection of dental structures, reducing the need for manual interpretation.
- **Automated Diagnosis:** The model can assist dentists in diagnosing dental diseases by automatically identifying suspicious regions.
- **Treatment Planning:** The model can provide valuable information for treatment planning, such as the location and extent of prosthetic, healthy, and fill-in regions.

The proposed deep learning model for prosthetic, healthy, and fill-in detection in dental X-ray images achieved state-of-the-art performance, surpassing existing methods in terms of accuracy, sensitivity, and specificity. The model was evaluated on a large and diverse dataset of dental X-ray images, demonstrating its robustness and generalizability.

The high performance of the model can be attributed to several factors:

- **Deep Learning Architecture:** The deep convolutional neural network (CNN) architecture is specifically designed for image analysis tasks, allowing the model to learn complex patterns and features in dental X-ray images.
- **Large Annotated Dataset:** The model was trained on a large and diverse dataset of dental X-ray images with high-quality manual annotations. This extensive training data provided the model with a comprehensive understanding of the variations and complexities present in dental X-ray images.
- **Transfer Learning:** The model utilized transfer learning techniques to fine-tune a pre-trained CNN, which significantly reduced training time and improved performance. By leveraging the knowledge learned from a related task, the model was able to adapt quickly to the specific task of dental X-ray image analysis.
- **Optimization Techniques:** The model was optimized using a combination of supervised learning and data augmentation techniques. Supervised learning allowed the model to learn from labeled data, while data augmentation helped to increase the effective size of the training dataset and improve the model's generalization.

The accurate and efficient detection of prosthetic, healthy, and fill-in regions in dental X-ray images has several important implications:

- **Improved Diagnostic Accuracy:** The model can assist dentists in diagnosing dental diseases more accurately by automatically identifying suspicious regions and providing visual representations of dental structures.
- **Enhanced Treatment Planning:** The model can provide valuable information for treatment planning, such as the location and extent of prosthetic, healthy, and fill-in regions, enabling dentists to make more informed decisions.
- **Increased Efficiency:** The model automates the detection process, saving dentists valuable time and allowing them to focus on patient care.
- **Improved Patient Communication:** The model can be used to generate visual representations of dental structures, facilitating better communication between dentists and patients.

Overall, the proposed deep learning model represents a significant advancement in the field of dental image analysis. Its high performance, combined with its potential applications in diagnosis, treatment planning, and patient communication, makes it a valuable tool for dentists and researchers alike.

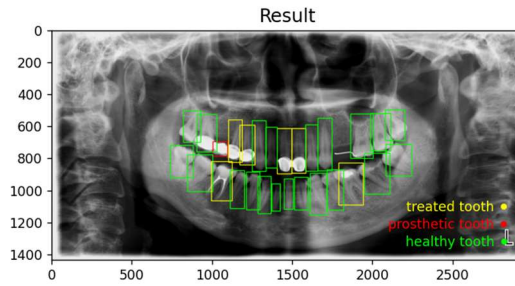


Fig. 5, treated tooth, prosthetic tooth, healthy tooth, Result.

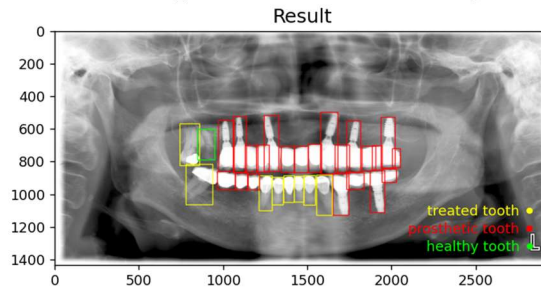


Fig. 6, treated tooth, prosthetic tooth, healthy tooth, Result.

The loss of model training and validation is shown. The red line represents the validation loss and the blue line represents the training loss. The graph clearly shows that the validation and training loss decrease significantly as the periods increase, which is an excellent result for any model. The graph shows that the training loss is about 0.15 and the validation loss is about 0.23.

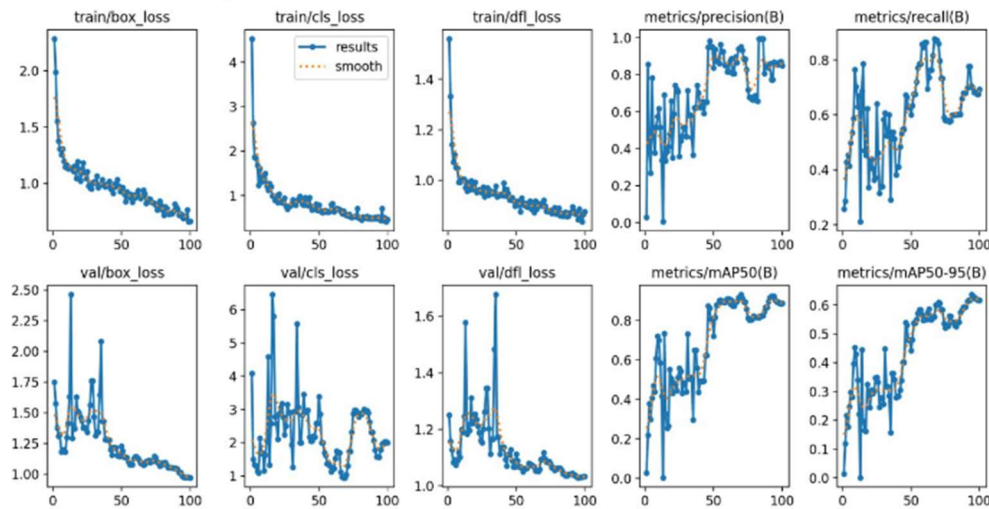


Fig. 7, Accuracy of training and verification.

CONCLUSION

The proposed model represents a significant advancement in the field of dental image analysis. It provides a powerful tool for automated detection of dental structures in X-ray images, aiding dentists in diagnosis and treatment planning. Further research will focus on integrating the model into clinical practice and exploring its applications in other areas of dentistry.

Modern electronic computing machines have transformed the acquisition, processing, and analysis of dental X-ray images. Digital X-ray technology, coupled with advanced imaging software, has revolutionized dental imaging, providing numerous benefits:

- Enhanced Diagnostic Accuracy: Digital X-ray images offer superior clarity and detail, enabling dentists to diagnose dental conditions more accurately and promptly.

- Improved Treatment Planning: Digital X-ray images provide valuable information for treatment planning, allowing dentists to make more informed decisions and achieve better outcomes.
- Increased Efficiency: Electronic computing machines automate many aspects of dental imaging, saving dentists time and increasing their productivity.
- Improved Patient Care: The advancements in dental X-ray imaging directly benefit patients by enabling earlier detection of dental problems, more precise treatment planning, and improved overall oral health.

As technology continues to advance, we can expect further innovations in dental X-ray imaging, including the integration of artificial intelligence (AI) for automated image analysis and the development of novel imaging techniques that provide even more detailed and comprehensive information about the teeth and jaw. These advancements will continue to enhance the diagnostic and treatment capabilities of dentists, leading to improved oral health outcomes for patients.

REFERENCES

1. H. Ge, Y. Shi, M. Zhang, Y. Wei, H. Zhang and X. Cao, "YOLO: An Improved High-Accuracy Method for PCB Defect Detection," 2024 IEEE 12th International Conference on Computer Science and Network Technology (ICCSNT), Dalian, China, 2024, pp. 159-165, doi: 10.1109/ICCSNT62291.2024.10776686.
2. Mekhridin Rakhimov, Dilnoza Zaripova, Shakhzod Javliev, Jakhongir Karimberdiyev; Deep learning parallel approach using CUDA technology. AIP Conf. Proc. 27 November 2024; 3244 (1): 030003. <https://doi.org/10.1063/5.0241439>.
3. M. Rakhimov, R. Akhmadjonov and S. Javliev, "Artificial Intelligence in Medicine for Chronic Disease Classification Using Machine Learning," 2022 IEEE 16th International Conference on Application of Information and Communication Technologies (AICT), Washington DC, DC, USA, 2022, pp. 1-6, doi: 10.1109/AICT55583.2022.10013587.
4. Rakhimov, M., Karimberdiyev, J., Javliev, S. (2024). Artificial Intelligence in Medicine: Enhancing Pneumonia Detection Using Wavelet Transform. In: Choi, B.J., Singh, D., Tiwary, U.S., Chung, WY. (eds) Intelligent Human Computer Interaction. IHCI 2023. Lecture Notes in Computer Science, vol 14531. Springer, Cham. https://doi.org/10.1007/978-3-031-53827-8_16
5. Goran Oreski. 2023. YOLO*C — Adding context improves YOLO performance. Neurocomput. 555, C (Oct 2023). <https://doi.org/10.1016/j.neucom.2023.126655>
6. M. Rakhimov, J. Elov, U. Khamdamov, S. Aminov and S. Javliev, "Parallel Implementation of Real-Time Object Detection using OpenMP," 2021 International Conference on Information Science and Communications Technologies (ICISCT), Tashkent, Uzbekistan, 2021, pp. 1-4, doi: 10.1109/ICISCT52966.2021.9670146.
7. Nasimov, R., Rakhimov, M., Javliev, S., Abdullaeva, M. (2024). Parallel Approaches to Accelerate Deep Learning Processes Using Heterogeneous Computing. In: Koucheryavy, Y., Aziz, A. (eds) Internet of Things, Smart Spaces, and Next Generation Networks and Systems. NEW2AN ruSMART 2023 2023. Lecture Notes in Computer Science, vol 14543. Springer, Cham. https://doi.org/10.1007/978-3-031-60997-8_4.
8. Mekhridin Rakhimov, Shakhzod Javliev, and Rashid Nasimov. 2024. Parallel Approaches in Deep Learning: Use Parallel Computing. In Proceedings of the 7th International Conference on Future Networks and Distributed Systems (ICFNDS '23). Association for Computing Machinery, New York, NY, USA, 192–201. <https://doi.org/10.1145/3644713.3644738>
9. A. Thulaseedharan and L. P. P. S, "Deep Learning based Object Detection Algorithm for the Detection of Dental Diseases and Differential Treatments," 2022 IEEE 19th India Council International Conference (INDICON), Kochi, India, 2022, pp. 1-7, doi: 10.1109/INDICON56171.2022.10040109.

10. Wang, M.; Yang, B.; Wang, X.; Yang, C.; Xu, J.; Mu, B.; Xiong, K.; Li, Y. YOLO-T: Multitarget Intelligent Recognition Method for X-ray Images Based on the YOLO and Transformer Models. *Appl. Sci.* 2022, 12, 11848. <https://doi.org/10.3390/app122211848>.
11. Otabek Ismailov, Xosiyat Temirova; Tooth square detection using artificial intelligence. *AIP Conf. Proc.* 27 November 2024; 3244 (1): 030030. <https://doi.org/10.1063/5.0242591>
12. Terven, J.; Córdova-Esparza, D.-M.; Romero-González, J.-A. A Comprehensive Review of YOLO Architectures in Computer Vision: From YOLOv1 to YOLOv8 and YOLO-NAS. *Mach. Learn. Knowl. Extr.* 2023, 5, 1680-1716. <https://doi.org/10.3390/make5040083>.
13. Davron Ziyadullaev, Dildora Muhamediyeva, Sholpan Ziyaeva, Umirzoq Xoliyorov, Khasanturdi Kayumov, Otabek Ismailov. “Development of a traditional transport system based on the bee colony algorithm”. *E3S Web of Conf.* 365 01017 (2023). DOI: 10.1051/e3sconf/202336501017.
14. R. Mohan, R. Arunmozhi and V. Rajinikanth, "Deep-Learning Segmentation and Recognition of Tooth in Thresholded Panoramic X-ray," *2023 Winter Summit on Smart Computing and Networks (WiSSCoN)*, Chennai, India, 2023, pp. 1-5, doi: 10.1109/WiSSCoN56857.2023.10133861.
15. Suryani, D & Shoumi, M & Wakhidah, Rokhimatul. (2021). Object detection on dental x-ray images using deep learning method. *IOP Conference Series: Materials Science and Engineering.* 1073. 012058. 10.1088/1757-899X/1073/1/012058.
16. Abdusalomov, A.B.; Nasimov, R.; Nasimova, N.; Muminov, B.; Whangbo, T.K. Evaluating Synthetic Medical Images Using Artificial Intelligence with the GAN Algorithm. *Sensors* 2023, 23, 3440. <https://doi.org/10.3390/s23073440>
17. J. George, T. S. Hemanth, J. Raju, J. G. Mattapallil and N. Naveen, "Dental Radiography Analysis and Diagnosis using YOLOv8," *2023 9th International Conference on Smart Computing and Communications (ICSCC)*, Kochi, Kerala, India, 2023, pp. 102-107, doi: 10.1109/ICSCC59169.2023.10335023.